Electronic Supplementary Material (ESI) for RSC Advances.

Mild fabrication of silica-silver nanocomposites as active platforms for environmental remediation

A. Mignani,[a*] S. Fazzini,[b] B. Ballarin,[b*] E. Boanini,[c] M. C. Cassani,[b] C. Maccato,[d] D. Barreca,[e] D. Nanni[b]

[a] *Center for Industrial Research - Advanced Applications in Mechanical Engineering and Materials Technology (CIRI-MAM), University of Bologna, Viale del Risorgimento, 2 I-40136 Bologna, Italy*

[b] *Department of Industrial Chemistry "Toso Montanari", University of Bologna and INSTM, Viale del Risorgimento, 4 I-40136 Bologna, Italy*

[c] *Department of Chemistry "Giacomo Ciamician", University of Bologna, Via Selmi, 2 I-40126 Bologna, Italy*

[d] *Department of Chemical Sciences, University of Padova and INSTM, Via Marzolo 1, I-35131 Padova, Italy*

[e] *CNR-IENI and INSTM, c/o Department of Chemical Sciences, University of Padova, Via Marzolo 1, I-35131 Padova, Italy*

[*]corresponding authors e-mail addresses: barbara.ballarin@unibo.it; a.mignani@unibo.it tel.: +390512093704; fax: +390512093690

SUPPORTING INFORMATION

List of Abbreviations:

Ag_{NPS}: Silver nanoparticles

AZ: Azorubine

BE: binding energy

BET: Brunauer-Emmett-Teller specific surface area analysis by gas adsorption

DLS: dynamic light scattering

FE-SEM: Field Emission-Scanning Electron Microscopy

FWHM: Full Width at Half Maximum

LMB: Leuco Methylene Blue

MB: Methylene blue

$NaBH_4$: Sodium Borohydride

NH_4OH: Ammonia Hydroxide Solution

SiO_2-PEI: Polyethylenimine-functionalized silica beads

SY: Sunset Yellow

UV-Vis: Ultraviolet–visible spectroscopy

XPS: X-ray Photoelectron

XE-AES: X-ray Excited Auger Electron Spectroscopy

XRD: X-ray Diffraction

XRF: X-ray fluorescence

1. XRD analysis

The presence of chlorides (present as impurity) in the commercial SiO_2-PEI beads causes problems during the AgNPs/SiO_2-PEI preparation, giving rise to silver chloride precipitation as shown by XRD pattern (see figure S1).

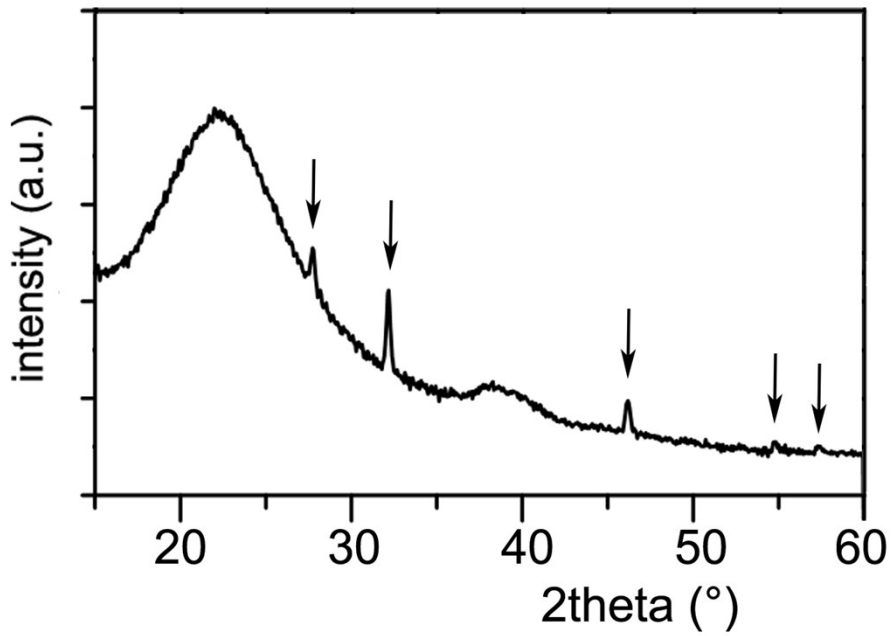

Fig. S1. XRD pattern of catalyst samples without pre-treatment in 1.3 M KNO_3.

2. XPS and XE-AES analyses

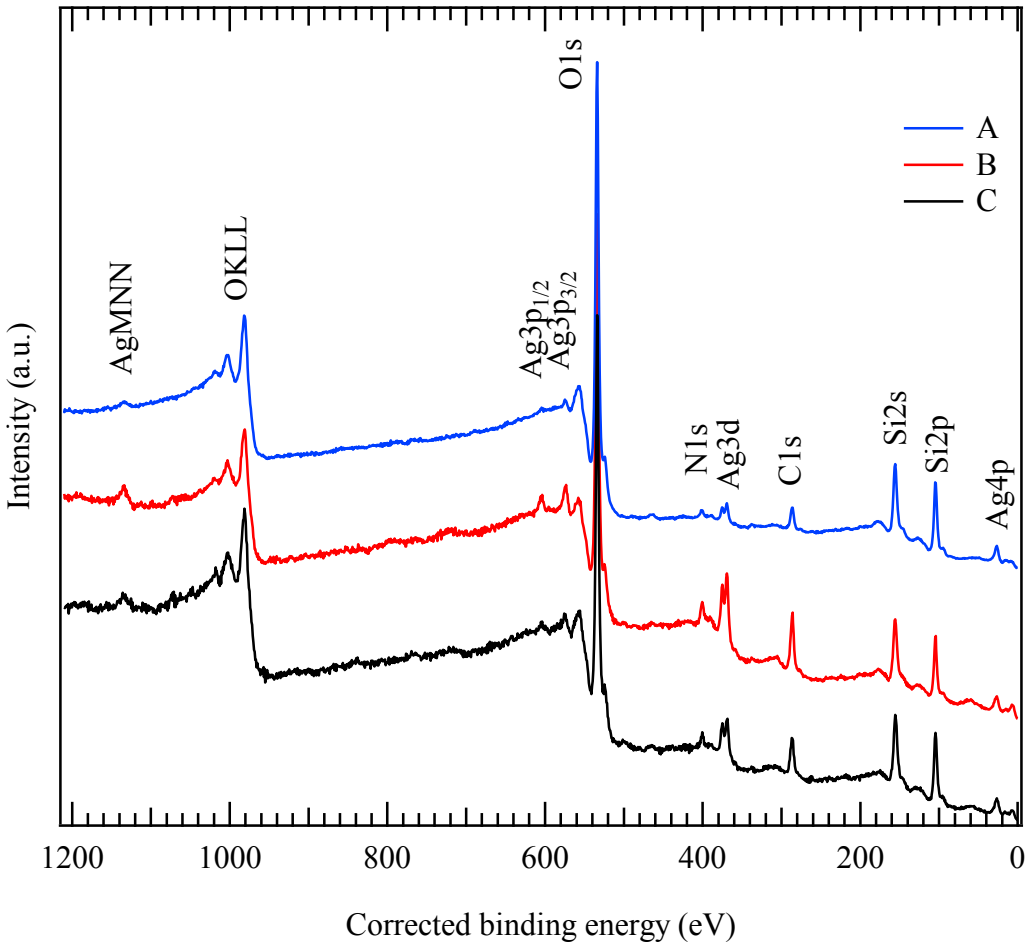

Fig. S2. Surface survey spectra of AgNPs/(SiO_2-PE-2) samples: A) before catalysis; B) after Methylene blue (MB) catalysis and C) after Sunset Yellow (SY) catalysis.

The survey spectra of the analyzed samples (**Fig. S2**) are qualitatively very similar and indicate the presence of carbon, oxygen, silver, silicon and nitrogen. No other elements were detected in appreciable amounts.

Fig. S3 displays the higher resolution surface C1s, O1s, Ag3d, Si2s, N1s and AgMNN regions, whose analysis allowed a more detailed insight into the sample composition.

Atomic percentage values are reported in **Table S1**.

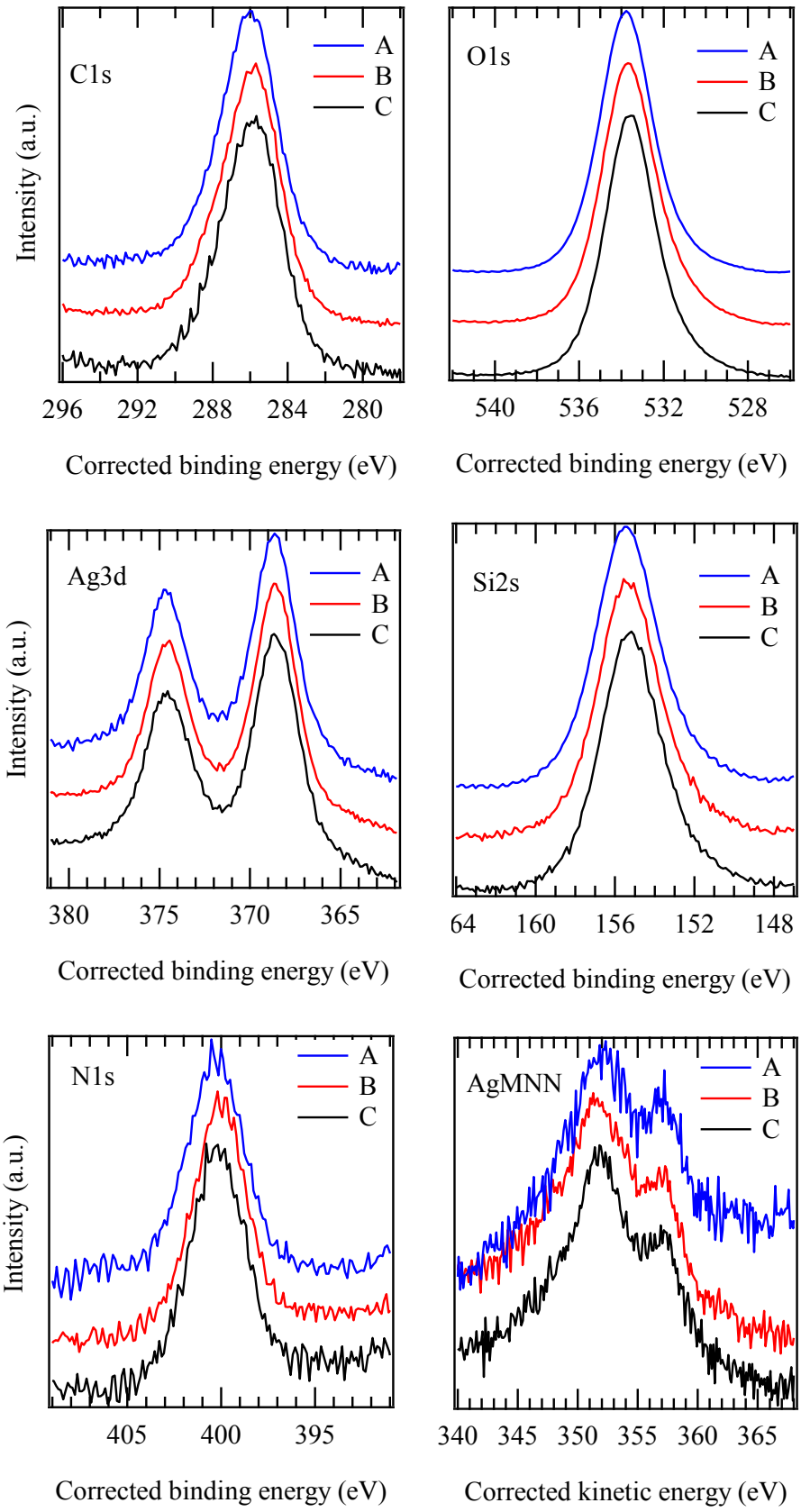

Fig. S3. Higher resolution XPS surface signals collected for the analyzed specimens.

Table S1. Atomic percentages for AgNPs/(SiO_2-PE-2) samples before (A) and after catalysis (B and C). The O/Si and Ag/Si atomic ratios are also provided. The 3 specimens present a rather similar O/Si ratio, but different carbon contents and different Ag/Si ratios.

A: AgNPs/(SiO_2-PEI-2) before catalysis	**C**	**O**	**Ag**	**Si**	**N**
%	9.3	61.8	0.6	26.5	1.8
O/Si = 2.3			Ag/Si = 0.02		

B: AgNPs/(SiO_2-PEI-2) after MB catalysis	**C**	**O**	**Ag**	**Si**	**N**
%	20.8	51.6	1.9	21.1	4.5
O/Si = 2.4			Ag/Si = 0.1		

C: AgNPs/(SiO_2-PEI-2) after SY catalysis	**C**	**O**	**Ag**	**Si**	**N**
%	14.9	55.8	1.3	24.8	3.1
O/Si = 2.2			Ag/Si = 0.05		

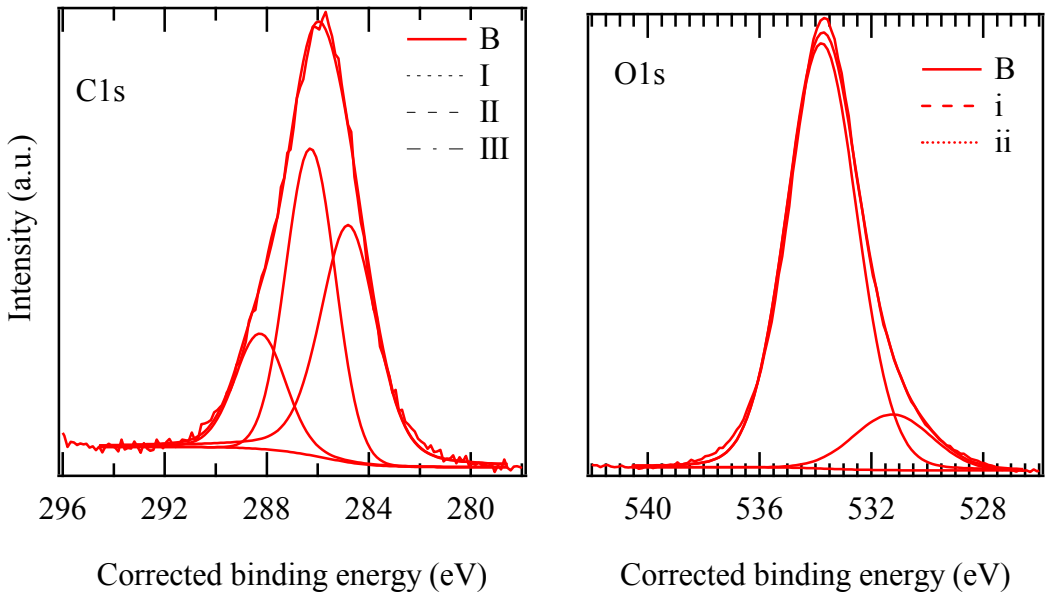

Fig. S4. Peak fitting for C1s and O1s signals in the case of sample B: AgNPs/(SiO2-PEI-2) after MB catalysis.

A detailed analysis of the peak shape and energy position yielded similar results for A, B and C. As an example, Fig. S4 displays the curve fitting results for C1s and O1s signals in the case of B: AgNPs/(SiO_2-PEI-2) after MB catalysis. The C1s photopeak could be decomposed by means of three distinct components: i, located at 284.8 eV [Full Width at Half Maximum (FWHM) = 2.6 eV, 41.8% of the total C amount], related to adventitious carbon, aliphatic residuals in PEI and C-C bonds in MB residuals adsorbed on the system surface [1,2]; ii, located at 286.3 eV (FWHM = 2.3 eV, 41.2% of the total C amount), mainly related to C-N bonds in PEI and in MB residuals adsorbed on the system surface [1]; iii, located at 288.2 eV (FWHM = 2.3 eV, 17.0% of the total C amount), mainly related to carbonate/bicarbonate species arising from atmospheric exposure [4,5]. The O1s peak was fitted by two different bands: i, BE = 533.8 eV (FWHM = 3.0 eV, 87.8% of the total O amount), the majority contibuting component, related to silica [1]; ii, BE = 531.2 eV (FWHM = 3.3 eV, 12.2% of the total O amount), related to silver carbonates/bicarbonates, in

accordance with the literature [4,5]. Nevertheless, it is also worth noticing that other species could be responsible for the latter band, including hydroxyl groups and adsorbed O_2 [4]. The presence of these species was responsible for an O/Si atomic ratio slightly higher than that expected for stoichiometric SiO_2 (compare Table S1).

Irrespective of the treatment conditions, the Ag 3d peak was always characterized by a single doublet, with the $Ag3d_{5/2}$ component located at 368.5 eV (average FWHM = 2.9 eV), suggesting the presence of metallic silver [6]. Nevertheless, the evaluation of the silver Auger parameters [α_1 = $BE(Ag3d_{5/2}) + KE(M_5NN)$; $\alpha_2 = BE(Ag3d_{5/2}) + KE(M_4NN)$] is necessary since the chemical shift of the Ag3d peak alone does not allow an unambiguous distinction among the various Ag chemical states [2-4,7]. In the present case, the calculation yielded the following average values: α_1 = 720.2 eV; α_2 = 725.6 eV, intermediate values between those expected for Ag(0) and Ag(I) [5,8,9]. This result agrees with the minority presence of oxidized Ag species, such as carbonate-related ones, in accordance with C1s spectral features (see above). A reliable quantitative evaluation of the relative Ag(0) and Ag(I) amounts by Ag 3d peak deconvolution is prevented by the very close BEs for the two oxidation states [2].

For a more accurate quantification of the relative Ag/Si content, the Si2s signal was recorded instead of the Si2p one [5]. The Si 2s features (average BE = 155.3 eV; average FWHM = 3.8 eV) were in agreement with SiO_2 presence [1].

The interpretation of the increase in the Ag/Si ratio after catalytic experiments can be performed by taking into account the FE-SEM images (see Fig. S8), that display an increase in the Ag-containing particle size from 9 to 19 nm after catalytic tests. This size variation could be traced back to a re-organization of silver particle distribution in the target materials, and, in particular, to segregation phenomena of Ag-based NPs in the outermost system layers after catalysis. The occurrence of such a process could explain both the increase in silver NP size and the higher Ag/Si ratio determined by

XPS analyses after catalytic tests.

The N1s peak (average BE = 400.2 eV, average FWHM = 3.3 eV) was in agreement with the presence of C-N moieties in PEI [1].

3 Methylene blue catalysis

Table S2. Comparison of kinetic constant values employed in the catalytic degradation of MB, reported in literature.

	k **(10^{-2} s^{-1})**	**Reference**
AgNPs by *Saraca indica Flore*	2.80	[10]
	0.74	
Biosynthesized AgNPs	0.25	[11]
	0.37	
Au@TiO_2 nanocomposites	0.26	[12]
AgNPs by *Trigonella foenum-*	1.70	[13]
graecum	1.19	
	0.81	

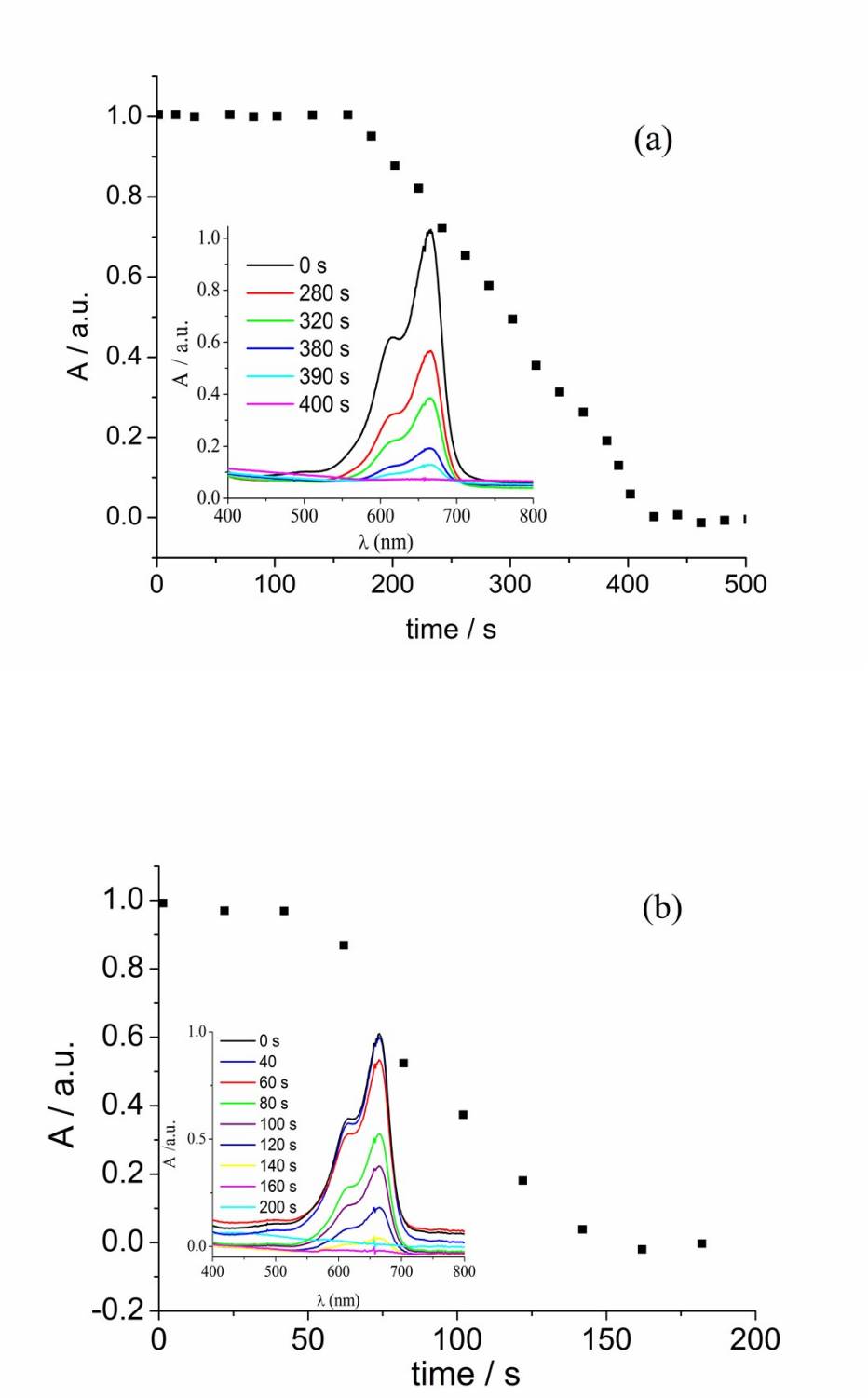

Figure S5. Evolution of absorbance at λ_{max} during the reduction of MB by $NaBH_4$ in presence of AgNPs/(SiO_2-PEI-2) at: (a) 1/8/425; (b) 1/8/1700 MB/Ag/$NaBH_4$ molar ratio. In the inset: the corresponding plot of A vs λ.

4. UV-Vis spectra of Sunset Yellow (SY) and Azorubine (AZ)

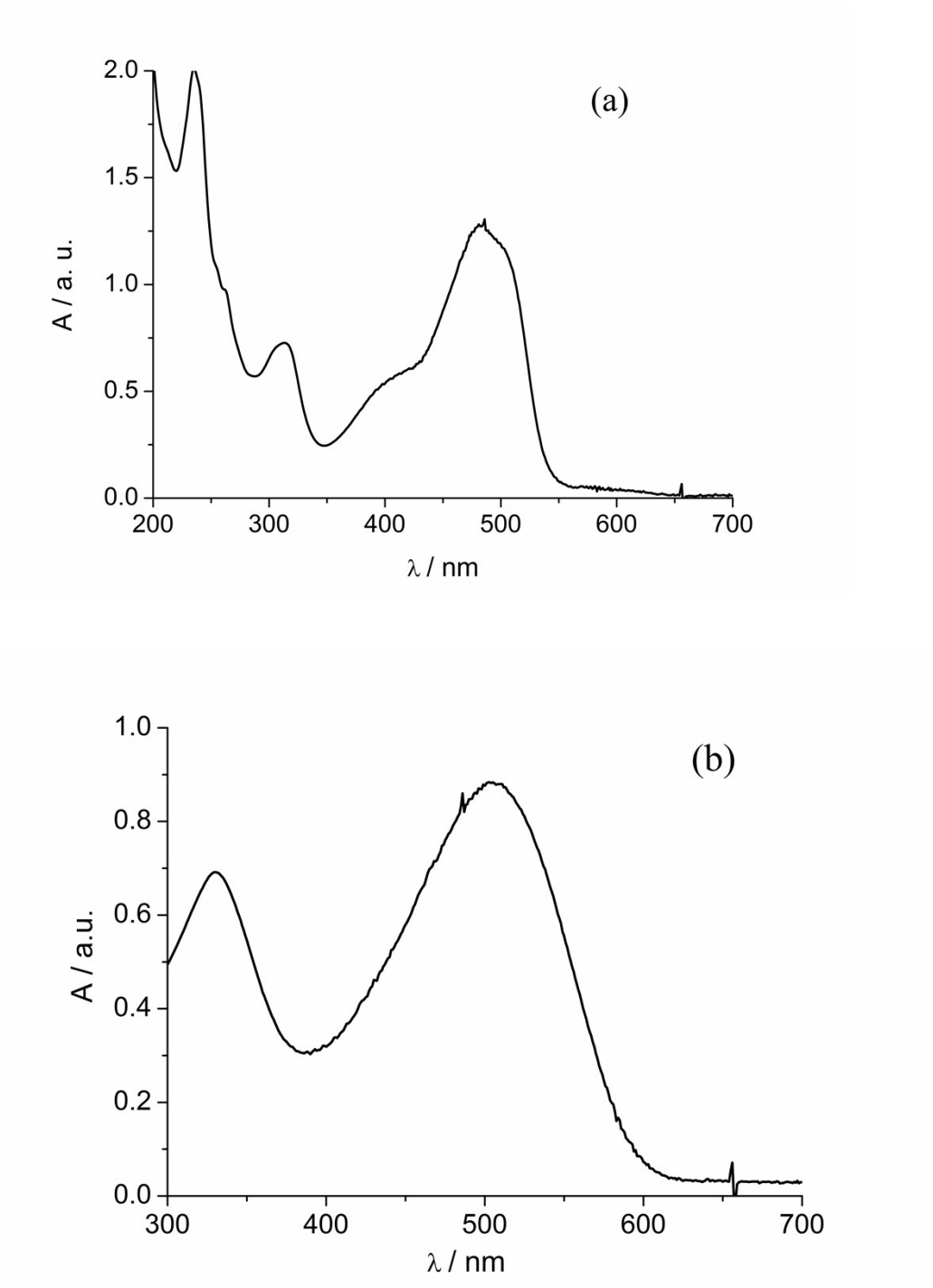

Figure S6. UV-Vis spectra of (a) sunset yellow (SY) and (b) azorubine (AZ).

5. Catalytic reduction of azo dyes SY and AZ by AgNPs/(SiO_2-PEI-2)

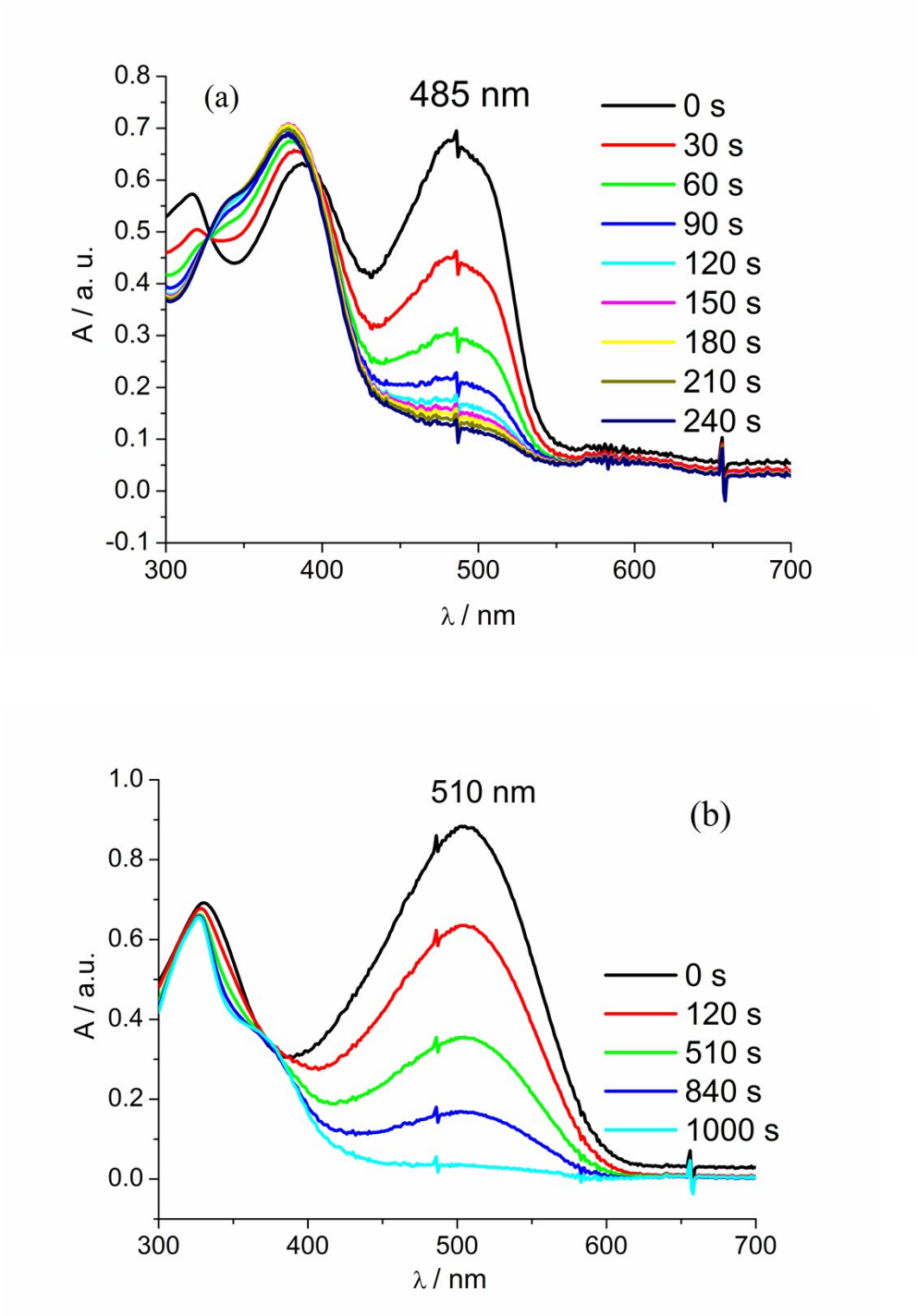

Figure S7. Evolution of UV-Vis absorption spectra of (a) SY and (b) AZ by $NaBH_4$ in presence of AgNPs/(SiO_2-PEI-2) at 1/4/21 Dye/Ag/$NaBH_4$ molar ratio.

6. SEM analysis

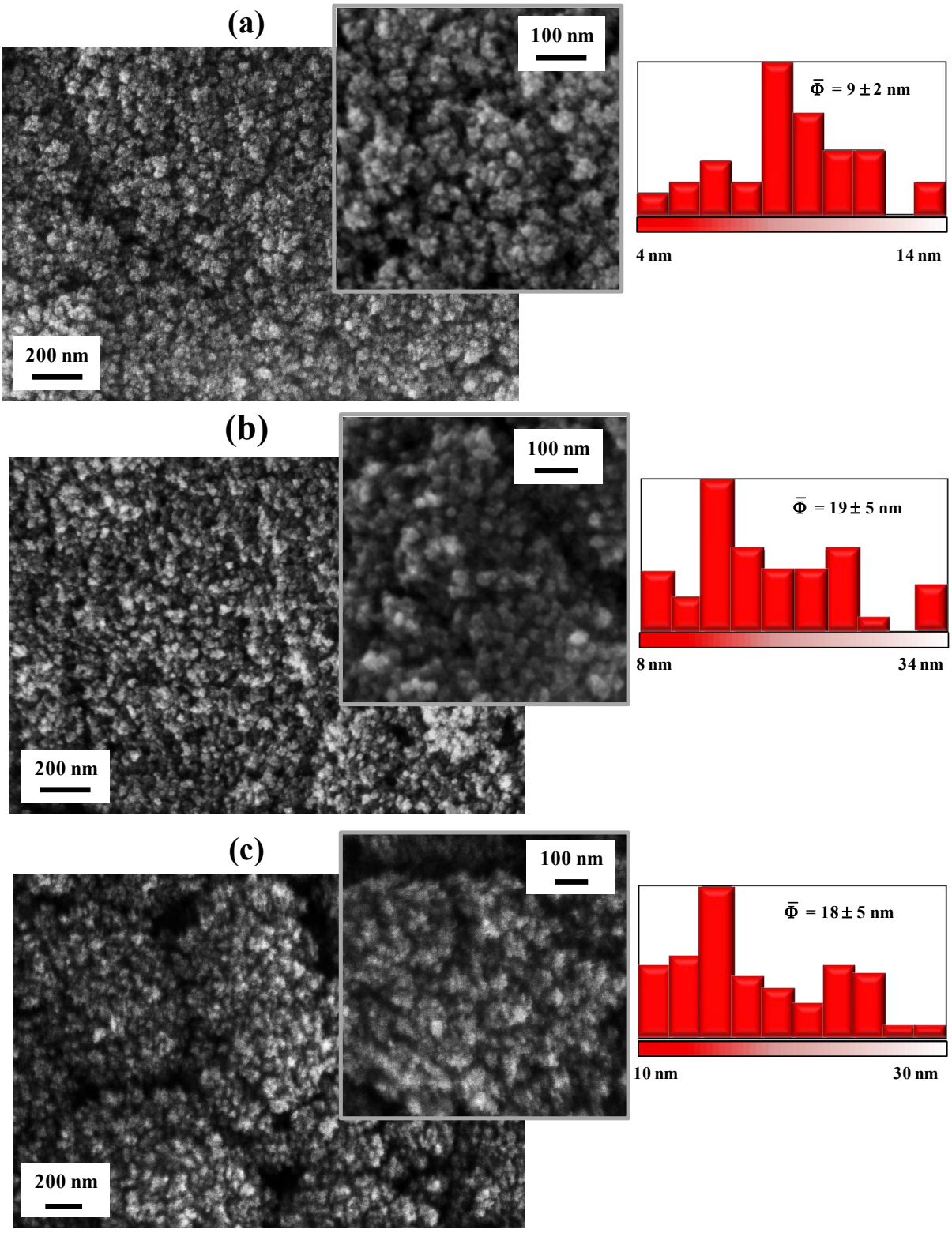

Figure S8. FE-SEM images of AgNPs/(SiO_2-PEI-2): (a) before catalysis; (b) after MB catalysis; (c) after SY catalysis.

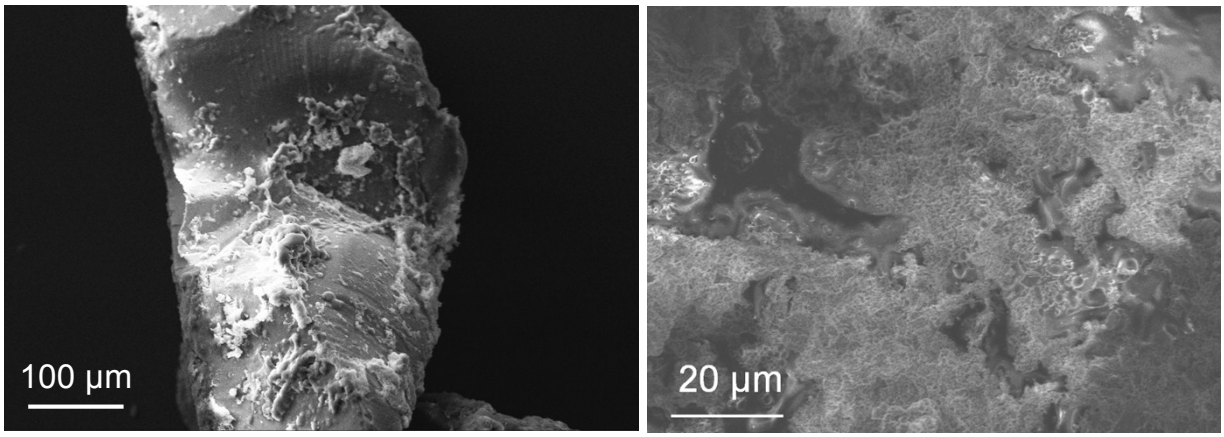

Figure S9. SEM images of commercial SiO_2-PEI at different magnification.

7. UV-Vis spectra of MB before and after addition of AgNPs/(SiO_2-PEI-2)

In order to evaluate the amount of the adsorbed dyes on AgNPs/(SiO_2-PEI-2) before the catalytic reaction a comparison of the UV-Vis absorption spectra of a MB solution was made. The UV-Vis spectrum of MB solution was registered before and after 3600 s from the addition of AgNPs/(SiO_2-PEI-2) (1/12 MB/Ag molar ratio) in absence of $NaBH_4$. From the absorbance decrease a value of 10% of adsorbed MB could be estimated.

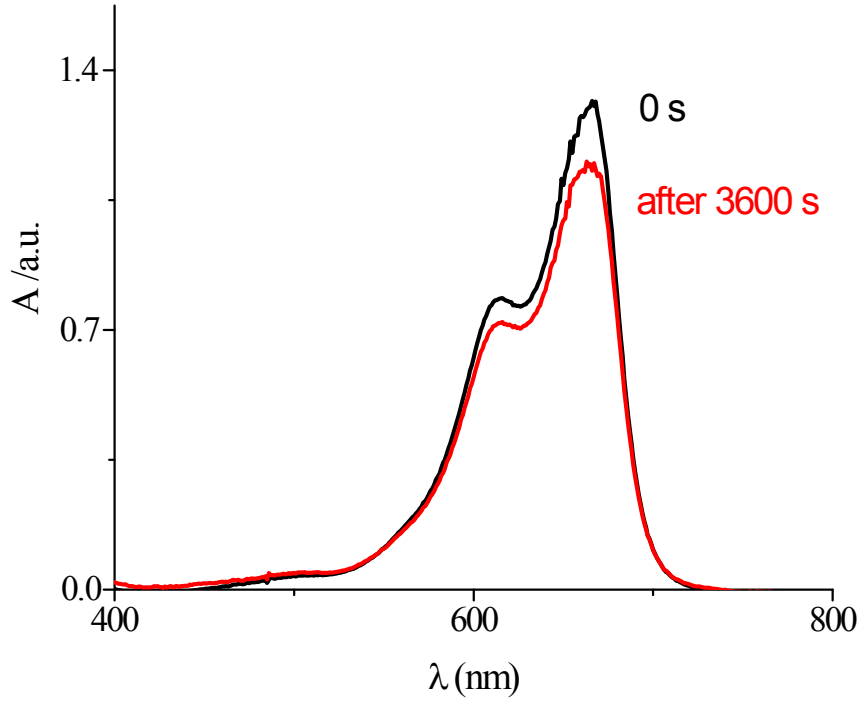

Figure S10 UV-Vis absorption spectra of a MB solution before and after 3600 s from the addition of AgNPs/(SiO_2-PEI-2) (1/12 MB/Ag molar ratio) in absence of $NaBH_4$.

References

[1] http://srdata.nist.gov/xps.

[2] Moulder, J. F.; Stickle, W. F.; Sobol, P. E.; Bomben, K. D. *Handbook of X-ray Photoelectron Spectroscopy*, edited by J. Chastain (Perkin Elmer Corporation, Eden Prairie, MN, 1992.

[3] Briggs, D.; Seah, M. P. *Practical Surface Analysis by Auger and X-ray Photoelectron Spectroscopy*, J. Wiley & Sons,1983.

[4] Barreca, D.; Gasparotto, A.; Maragno, C.; Tondello, E.; Gialanella, S. *J. Appl. Phys.* 2005, **97**, 054311.

[5] Armelao, L.; Barreca, D.; Bottaro, G.; Gasparotto, A.; Maragno, C.; Tondello, E. *Surface Science Spectra* 2003, **10**, 170.

[6] Salaita, G. N. ; Hazos, Z. F.; Hoflund, G. B. *J. Electron Spectrosc. Relat. Phenom.* 2000, **107**, 73.

[7] Armelao, L. ; Barreca, D.; Bottaro, G.; Gasparotto, A.; Maccato, C.; Tondello, E.; Lebedev, O. I.; Turner, S.; Van Tendeloo, G.; Sada, C.; Lavrenčič Štangar, U. *Chem. Phys. Chem.* 2009, **10**, 3249.

[8] De, G.; Licciulli, A.; Massaro, C.; Tapfer, L.; Catalano, M.; Battaglin, G.; Meneghini, C.; Mazzoldi, P. *J. Non-Cryst. Solids* 1996, **194***,* 225.

[9] Simon, Q.; Barreca, D.; Bekermann, D.; Gasparotto, A.; Maccato, C.; Comini, E.; Gombac, V.; Fornasiero, P.; Lebedev, O.I. ; Turner, S.; Devi, A.; Fischer, R. A.; Van Tendeloo, G. *International Journal of Hydrogen Energy*, 2011, **36**, 15527.

[10] Vidhu, V. K.; Philip, D. Spectroscopic, microscopic and catalytic properties of silver nanoparticles synthesized using Saraca indica flore. *Spectrochimica Acta Part A: Molecular and Biomolecular Spectroscopy* 2014, **117**, 102.

[11] Suvith, V. S.; Philip, D. Catalytic degradation of methylene blue using biosynthesized gold and silver nanoparticles. *Spectrochimica Acta Part A: Molecular and Biomolecular Spectroscopy* 2014, **118**, 526.

[12] Khan, M. M.; Lee, J.; Cho, M. H. Au@TiO_2 nanocomposites for the catalytic degradation of methyl orange and methylene blue: An electron relay effect. *Journal of Industrial and Engineering Chemistry* 2014, **20***,* 1584.

[13] Vidhu, V. K.; Philip, D. Catalytic degradation of organic dyes using biosynthesized silver Nanoparticles. *Micron* 2014, **56**, 54.